BRAIN
ORIGINAL ARTICLE

Distinct virtual histology of grey matter atrophy in four neuroinflammatory diseases

Jun Sun,[1,2,†] Min Guo,[1,2,†] Li Chai,[1,2,†] Siyao Xu,[1,2,†] Yuerong Lizhu,[1,2] Yuna Li,[1,2] Yunyun Duan,[1,2] Xiaolu Xu,[1,2] Shan Lv,[1,2] Jinyuan Weng,[3] Kuncheng Li,[4] Fuqing Zhou,[5] Haiqing Li,[6] Yongmei Li,[7] Xuemei Han,[8] Fu-Dong Shi,[9,10] Xinghu Zhang,[11] De-Cai Tian,[11,‡] Zhizheng Zhuo[1,2,‡] and Yaou Liu[1,2,‡]

[†,‡]These authors contributed equally to this work.

Grey matter (GM) atrophies are observed in multiple sclerosis, neuromyelitis optica spectrum disorders [NMOSD; both anti-aquaporin-4 antibody-positive (AQP4+) and -negative (AQP4–) subtypes] and myelin oligodendrocyte glycoprotein antibody-associated disease (MOGAD). Revealing the pathogenesis of brain atrophy in these disorders would help their differential diagnosis and guide therapeutic strategies.

To determine the neurobiological underpinnings of GM atrophies in multiple sclerosis, AQP4+ NMOSD, AQP4– NMOSD and MOGAD, we conducted a virtual histology analysis that links T1-weighted image derived GM atrophy and gene expression using a multicentre cohort of 324 patients with multiple sclerosis, 197 patients with AQP4+ NMOSD, 75 patients with AQP4– NMOSD, 47 patients with MOGAD and 2169 healthy control subjects. First, interregional GM atrophy profiles across the cortical and subcortical regions were determined using Cohen's *d* between patients with multiple sclerosis, AQP4+ NMOSD, AQP4– NMOSD or MOGAD and healthy controls. The GM atrophy profiles were then spatially correlated with the gene expression levels extracted from the Allen Human Brain Atlas, respectively. Finally, we explored the virtual histology of clinical-feature relevant GM atrophy using a subgroup analysis that stratified by physical disability, disease duration, number of relapses, lesion burden and cognitive function.

Multiple sclerosis showed a severe widespread GM atrophy pattern, mainly involving subcortical nuclei and brainstem. AQP4+ NMOSD showed an obvious widespread pattern of GM atrophy, predominately located in occipital cortex as well as cerebellum. AQP4– NMOSD showed a mild widespread GM atrophy pattern, mainly located in frontal and parietal cortices. MOGAD showed GM atrophy mainly involving the frontal and temporal cortices. High expression of genes specific to microglia, astrocytes, oligodendrocytes and endothelial cells in multiple sclerosis, S1 pyramidal cells in AQP4+ NMOSD, as well as S1 and CA1 pyramidal cells in MOGAD, had spatial correlations with GM atrophy profile, while no atrophy profile-related gene expression was found in AQP4– NMOSD. Virtual histology of clinical feature-relevant GM atrophy pointed mainly to the shared neuronal and endothelial cells, among the four neuroinflammatory diseases.

The unique underlying virtual histology patterns were microglia, astrocytes and oligodendrocytes for multiple sclerosis; astrocytes for AQP4+ NMOSD; and oligodendrocytes for MOGAD. Neuronal and endothelial cells were shared potential targets across these neuroinflammatory diseases. These findings may help the differential diagnoses of these diseases and promote the use of optimal therapeutic strategies.

1 Department of Radiology, Beijing Tiantan Hospital, Capital Medical University, Beijing, 100070, P. R. China
2 Tiantan Image Research Center, China National Clinical Research Center for Neurological Diseases, Beijing, 100070, P. R. China

Received December 11, 2023. Revised March 24, 2024. Accepted April 11, 2024. Advance access publication May 4, 2024

3 Department of Medical Imaging Product, Neusoft, Group Ltd., Shenyang, 110179, P. R. China
4 Department of Radiology, Xuanwu Hospital, Capital Medical University, Beijing, 100053, P. R. China
5 Department of Radiology, The First Affiliated Hospital, Nanchang University, Nanchang, Jiangxi Province, 330006, P. R. China
6 Department of Radiology, Huashan Hospital, Fudan University, Shanghai, 200040, China
7 Department of Radiology, The First Affiliated Hospital of Chongqing Medical University, Chongqing, 400016, P. R. China
8 Department of Neurology, China–Japan Union Hospital of Jilin University, Changchun, Jilin Province, 130031, P. R. China
9 Basic and Translational Medicine Center, China National Clinical Research Center for Neurological Diseases, Beijing, 100070, P. R. China
10 Department of Neurology and Tianjin Neurological Institute, Tianjin Medical University General Hospital, Tianjin, 300052, P. R. China
11 Department of Neurology, Beijing Tiantan Hospital, Capital Medical University, Beijing, 100070, P. R. China

Correspondence to: Yaou Liu, MD, PhD
Department of Radiology, Beijing Tiantan Hospital
Capital Medical University, No.119, the West Southern 4th Ring Road
Fengtai District, Beijing, 100070, China
E-mail: liuyaou@bjtth.org

Keywords: virtual histology; grey matter atrophy; multiple sclerosis; NMOSD; MOGAD

Introduction

Brain atrophy occurs in neuroinflammatory demyelinating disorders including multiple sclerosis,[1-5] aquaporin-4 antibody seropositive (AQP4+) and seronegative (AQP4–) neuromyelitis optica spectrum disorders (NMOSD)[6-10] and myelin oligodendrocyte glycoprotein (MOG) antibody-associated disease (MOGAD).[11,12] In particular, grey matter (GM) atrophy occurs early and is associated with physical disability and cognitive impairment in these diseases.[3,11-14] Understanding the shared and distinct pathogenic mechanisms of GM atrophy in these disorders will contribute to their differential diagnoses and guide optimal therapeutic strategies, which remain limited.

Several lines of evidence from autopsy or biopsy tissue and/or experimental models have indicated disease-shared and -specific characteristics of GM pathology (including cortex, subcortex, brainstem and cerebellum) in these four neuroinflammatory disorders. However, these findings have been obtained from separate studies and need further validation.[3,6-16] Consistent with these pathological findings, previous MRI studies have also identified shared and specific GM atrophy characteristics in patients with multiple sclerosis, AQP4+ NMOSD and MOGAD.[3,12,13] Cortical GM atrophy is a common clinical phenomenon in these diseases, especially multiple sclerosis. Subcortical GM atrophy can also occur in multiple sclerosis (e.g. in the caudate, putamen, globus pallidus, hippocampus, amygdala, nucleus accumbens region and ventral diencephalon), AQP4+ NMOSD (e.g. in the hippocampus and nucleus accumbens region) and MOGAD (e.g. in the hippocampus).[14] Furthermore, GM atrophy of the cerebellum has been observed in multiple sclerosis and AQP4+ NMOSD but not in MOGAD. It has been reported that multiple sclerosis patients show brainstem atrophy when compared with NMOSD patients.[17] Few studies have focused on AQP4– NMOSD due to its high heterogeneity; therefore, its GM atrophy profile across whole brain regions remains undetermined. Moreover, although there have been several reports of regional GM atrophy, the underlying pathological mechanisms for these GM atrophy profiles has not yet been investigated systematically. Brain GM atrophy patterns and their underlying pathological changes across GM atrophy profiles remain unclear.

Specific cell types in GM layers play critical roles in volume loss.[16,18,19] These cells can be classified into neuronal cells (mostly pyramidal cells and interneurons) and non-neuronal cells (mostly glial cells, namely, microglia, astrocytes and oligodendrocytes).[20,21] In multiple sclerosis, cumulative neuropathological evidence indicates that immune cell activation leads to GM atrophy at the early disease stage, accounting for irreversible clinical disability.[1-5] Moreover, extensive GM atrophy (in the cerebral cortex, deep GM structures, cerebellum and brainstem) is related to glial pathology in multiple sclerosis (e.g. activation of microglia and astrocytes).[15] In AQP4+ NMOSD, oligodendrocytes play an important role in brain atrophy, while interactions between glia and neurons induce neuronal loss in cortical layers II–IV.[6-10] In MOGAD, cortical pathology generally correlates with microglial reactivity, as observed in multiple sclerosis.[11] Currently, the shared and distinct neurobiological underpinnings of GM atrophy profiles among the four diseases are not well determined, nor have their pathological mechanisms been extensively studied in an identical framework to make them comparable. Moreover, the associated pathological changes due to disease aggravation remain relatively unknown, because biopsies are usually unavailable.[15,22]

Recently, virtual histology methods have been developed to link macroscopic MRI with mesoscopic histological cell features.[23] They have revealed the contribution of CNS cell types to human cerebral morphology in both healthy populations and those with psychiatric disorders exclusively through MRI.[24-27] The use of virtual histology can facilitate our understanding of MRI-derived measures in a neurobiological context and increase the value of MRI for tracking clinical progression and therapeutic effects in certain CNS disorders.

The purpose of this study was to assess the neurobiological underpinnings of GM atrophy profiles in patients with multiple sclerosis, AQP4+ NMOSD, AQP4– NMOSD and MOGAD using a virtual histology approach and identify pathological changes in clinical feature-associated subgroups. Our findings may benefit differential diagnoses and guide optimal therapies.

Materials and methods

Study design

We recruited 2812 participants, including 324 relapsing remitting multiple sclerosis, 197 AQP4+ NMOSD, 75 AQP4– NMOSD and 47 MOGAD patients, along with 2169 healthy controls. All participants had 3D T1-weighted images available that were obtained from multiple centres in China (see Table 1 for details). T1-weighted images were used to estimate GM atrophy profiles (represented by Cohen's *d*) in patients with multiple sclerosis, AQP4+ NMOSD, AQP4– NMOSD and MOGAD compared with healthy controls. To examine the virtual histology of GM atrophy, the widely used Allen Human Brain Atlas[23-26] (AHBA; six donors aged 24–57 years) and single-cell RNA sequencing data from the mouse hippocampus and S1 area of the cerebral cortex[27] were applied to explore shared and distinct relationships between CNS cell type-associated gene expression levels and GM atrophy profiles.

This study was approved by the institutional review board of Beijing Tiantan Hospital, Capital Medical University (Beijing, China) (KY2019-050-02). Written or oral informed consent was obtained from each participant in accordance with the Declaration of Helsinki. The use of images and clinical data from other centres was approved by their local institutional review boards.

Estimation of interregional grey matter atrophy profiles

FreeSurfer (command: recon -all) was used to obtain GM volume. Quality control was conducted by a senior neuroradiologist (Y.D.) with more than 20 years of experience. Tissue volume was extracted from 41 regions (left hemisphere, including cortical and subcortical GM and GM of bilateral cerebellum and brainstem), as defined in the latest Desikan–Killiany atlas. Regional brain atrophy profiles were obtained using multiple linear regression analyses, which modelled the GM volume for each region as a function of disease diagnosis (healthy controls, multiple sclerosis, AQP4+ NMOSD, AQP4– NMOSD and MOGAD), age, age-squared, sex and site-specific covariates (including MRI scanner and acquisition protocol).[25] Intergroup differences in the GM volume of each brain region were analysed [*post hoc t*-test with significance denoted by a false discovery rate (FDR)-corrected *P*-value (P_{FDR}) < 0.05]. Cohen's *d* across brain regions of each disease group relative to healthy controls was regarded as the GM atrophy profile. Correlation between regional GM volumes and clinical variables were analysed by Spearman correlation. Details regarding GM atrophy estimation, statistical analysis and the main findings are provided in the Supplementary material (Supplementary Figs 1–3 and Supplementary Table 1).

Virtual histology

Virtual histology is an approach that establishes the connection between a MRI-derived profile (such as an interregional GM atrophy profile) with an interregional profile of cell-specific gene expression.[23-26] Gene expression data from the AHBA were first mapped to the 41 brain regions of the Desikan–Killiany atlas. Donor-to-median correlations in the AHBA were analysed to retain only genes that had consistent profiles among the six donors.[25,26] First, 12 349 genes (P_{FDR} < 0.05 in all six donors) were selected with a high similarity of interregional gene expression (detailed in the Supplementary material, 'Methods' section). Second, 3189 genes identified from single-cell RNA sequencing data from the mouse hippocampus and S1 area of the cerebral cortex were used to further select genes for analysis (*n* = 1948). These final selected genes

Table 1 The demographics of the participants in this study

Items	HC (*n* = 2169)	MS (*n* = 324)	AQP4+ NMOSD (*n* = 197)	AQP4– NMOSD (*n* = 75)	MOGAD (*n* = 47)	Overall (*n* = 2812)
Age, years						
Mean (SD)	45.4 (10.3)	35.0 (10.9)	41.7 (13.3)	41.2 (13.7)	35.1 (11.4)	43.6 (11.3)
Median [Min, Max]	47.0 [18.0, 60.0]	33.7 [18.0, 65.0]	42.2 [18.0, 65.0]	40.0 [18.0, 64.2]	33.0 [18.8, 59.0]	45.0 [18.0, 65.0]
Sex						
Female	1184 (54.6%)	122 (37.7%)	13 (6.6%)	17 (22.7%)	15 (31.9%)	1351 (48.0%)
Male	985 (45.4%)	202 (62.3%)	184 (93.4%)	58 (77.3%)	32 (68.1%)	1461 (52.0%)
Education, years						
Mean (SD)	15.7 (3.4)	13.0 (3.4)	11.2 (3.8)	12.6 (3.2)	11.4 (4.7)	13.2 (3.9)
Median [Min, Max]	16.0 [9.0, 22.0]	15.0 [5.0, 19.0]	12.0 [0, 16.0]	12.0 [6.00, 19.0]	12.0 [0, 16.0]	15.0 [0, 22.0]
Disease duration, months						
Mean (SD)	NA (NA)	47.6 (60.6)	61.5 (77.2)	45.7 (47.6)	38.9 (52.5)	51.3 (64.6)
Median [Min, Max]	NA [NA, NA]	24.0 [0.4, 438]	36.0 [0.5, 459]	25.7 [2.0, 207]	12.4 [0.4, 197]	24.7 [0.4, 459]
EDSS						
Mean (SD)	NA (NA)	2.48 (1.68)	4.01 (2.08)	3.38 (2.06)	2.62 (1.34)	3.09 (1.97)
Median [Min, Max]	NA [NA, NA]	2.00 [0, 7.50]	3.50 [0, 9.00]	3.00 [0, 8.00]	3.00 [0, 5.00]	3.00 [0, 9.00]
Number of relapses						
Mean (SD)	NA (NA)	2.97 (2.09)	3.26 (2.54)	3.29 (2.66)	2.38 (1.68)	3.09 (2.34)
Median [Min, Max]	NA [NA, NA]	3.00 [1.00, 13.00]	2.00 [1.00, 17.00]	3.00 [1.00, 12.00]	2.00 [1.00, 7.00]	2.00 [1.00, 17.00]
Lesion volume, mm^3						
Mean (SD)	NA (NA)	18 100 (30 600)	4410 (8370)	5410 (8840)	4395 (4967)	14000 (26 500)
Median [Min, Max]	NA [NA, NA]	9120 [4, 253 000]	1630 [42, 42 800]	1760 [124, 29 100]	1777 [106, 15 130]	5830 [4, 253 000]
MoCA						
Mean (SD)	28.10 (2.36)	26.20(3.55)	25.20 (4.42)	24.60 (3.12)	23.90 (5.89)	25.80 (4.12)
Median [Min, Max]	29.00 [21.00, 30.00]	27.00 [14.00, 30.00]	26.00 [11.00, 30.00]	25.00 [20.00, 30.00]	25.00 [10.00, 30.00]	27.00 [10.00, 30.00]

AQP4+/– = AQP4 antibody-positive/negative; EDSS = Expanded Disability Status Scale; HC = healthy control; NMOSD = neuromyelitis optica spectrum disorder; MoCA = Montreal Cognitive Assessment; MOGAD = MOG antibody-associated disease; NA = not applicable; SD = standard deviation.

were categorized into nine cell types: CA1 pyramidal cells, S1 pyramidal cells, interneurons, astrocytes, microglia, oligodendrocytes, mural cells, endothelial cells and ependymal cells.[27] Interregional profiles of cell-specific gene expression across these 41 regions were then correlated with interregional GM atrophy profiles for each cell type. The significance of this distribution was tested using a resampling approach from 100 000 random samples. This analysis was restricted to MRI profiles from the left hemisphere only (because of data availability in the AHBA).

Principal component analysis

Given the similarity of findings across the four inflammatory diseases by virtual histology, a principal component analysis (PCA) was used to collect intersession variations of GM atrophy profiles from the four neuroinflammatory diseases, whose correlated cell types were identified from the virtual histology of GM atrophy profiles. Variations in interregional GM atrophy profiles from multiple sclerosis, AQP4+ NMOSD, AQP4– NMOSD and MOGAD patients were used to identify shared and unique GM atrophy patterns using 'psych' in the R package. In addition, the collective variances (PCA results) were estimated by cell types identified from the virtual histology of the GM atrophy profiles of the four diseases.

Hierarchical clustering analysis

Considering the heterogeneity of the four neuroinflammatory diseases, hierarchical clustering was used to collect intrasession variations of GM atrophy profiles. GM atrophies in multiple sclerosis, AQP4+ NMOSD, AQP4– NMOSD and MOGAD were clustered into optimal subtypes using the hierarchical clustering method with the R packages 'NbClust', 'factoextra' and 'igraph'. Furthermore, the GM atrophy subtypes in the four diseases were estimated by cell types identified using the virtual histology method.

Virtual histology of grey matter atrophy based on clinical features

The virtual histology of GM atrophy profiles based on clinical features was analysed. This included physical disability, disease duration, number of relapses, lesion volume and cognitive function. For each disease, participants were combined into subgroups: low and high physical disabilities [Expanded Disability Status Scale (EDSS) threshold, 3], short and long disease duration (disease duration threshold, 3 years), monophasic and multiphasic relapse (relapse number threshold, 1), mild and severe lesion burdens (lesion volume threshold, 3000 mm^3) and cognitive preservation and impairment [integrated Montreal Cognitive Assessment (MoCA) Z-score threshold, −1.5 compared with healthy controls] based upon the previous literature and clinical features of the cohort (detailed in the Supplementary material, 'Methods' section).

Statistical analysis

The GM atrophies of neuroinflammatory diseases were analysed by ANOVA, adjusting for site-related effects, age, sex and intracranial volume, followed by between group comparisons (*post hoc* *t*-test, with significance denoted by $P_{FDR} < 0.05$). Cohen's *d* across brain regions of each disease group relative to healthy controls was regarded as the GM atrophy profile. Spearman correlation was conducted to investigate the relationship between GM atrophy and EDSS, disease duration, number of relapses, lesion volume and cognitive function. The PCA and hierarchical clustering analysis were applied to analyse the intersession and intrasession variations of GM atrophy among the four neuroinflammatory diseases. All the statistical analyses were conducted using R software. Statistical significance was defined as a two-sided $P_{FDR} < 0.05$ due to the exploratory nature of this study.

Results

According to the investigations of 2812 participants, we characterized the GM atrophy profiles in patients with multiple sclerosis, AQP4+ NMOSD, AQP4– NMOSD and MOGAD compared with healthy controls across 41 brain regions, including the cortex, subcortical nuclei, cerebellum and brainstem (Fig. 1, Supplementary Figs 1 and 2 and Supplementary Table 1).

Grey matter atrophy patterns in multiple sclerosis, AQP4+ and AQP4– NMOSD and MOGAD

In patients with multiple sclerosis, GM atrophy was obviously in subcortical nuclei, insula, frontal, temporal, parietal, occipital and limbic cortices, as well as brainstem. In patients with AQP4+ NMOSD, GM atrophy was found in subcortical nuclei and frontal, temporal, parietal, occipital and limbic cortices, as well as cerebellum. In patients with AQP4– NMOSD, GM atrophy was located in subcortical nuclei and frontal, temporal, parietal and limbic cortices. In patients with MOGAD, GM atrophy was observed in the frontal and temporal cortices (Fig. 1).

Multiple sclerosis showed a severe widespread GM atrophy pattern, mainly involving subcortical nuclei and brainstem. AQP4+ NMOSD showed an obvious widespread GM atrophy pattern, predominately located in occipital cortex as well as cerebellum. AQP4– NMOSD showed a mild widespread GM atrophy pattern, mainly located in frontal and parietal cortices. MOGAD showed GM atrophy mainly involving the frontal and temporal cortices (Fig. 1).

Virtual histology of atrophy profiles in multiple sclerosis, AQP4+ and AQP4– NMOSD and MOGAD

In the present study, a negative Cohen's *d* value delineated GM atrophy in the patients. Upregulated gene expression is assumed to play a significant role in the development of GM atrophy. In patients with multiple sclerosis, interregional variation in the expression of genes specific to microglia, astrocytes, oligodendrocytes and endothelial cells was negatively associated with the interregional GM atrophy profile ($-0.184 < r < -0.980$, $P_{FDR} < 10^{-5}$; Fig. 2 and Supplementary Table 2). In patients with AQP4+ NMOSD, inter regional variation in the expression of genes specific to S1 pyramidal cells was negatively associated with the interregional GM atrophy profile ($r = -0.132$, $P_{FDR} < 10^{-5}$; Fig. 2 and Supplementary Table 2). In patients with MOGAD, interregional variation in the expression of genes specific to CA1 and S1 pyramidal cells was negatively associated with the interregional GM atrophy profile ($-0.117 < r < -0.099$, $P_{FDR} < 10^{-5}$; Fig. 2 and Supplementary Table 2). No specific CNS cell types were associated with the GM atrophy profile in patients with AQP4– NMOSD.

Virtual histology of the principal component analysis and hierarchical clustering results

The PCA results showed that the first and second principal components (PC1 and PC2) accounted for 47.4% and 26.2% of the variance in different GM atrophy profiles, respectively (Fig. 3A).

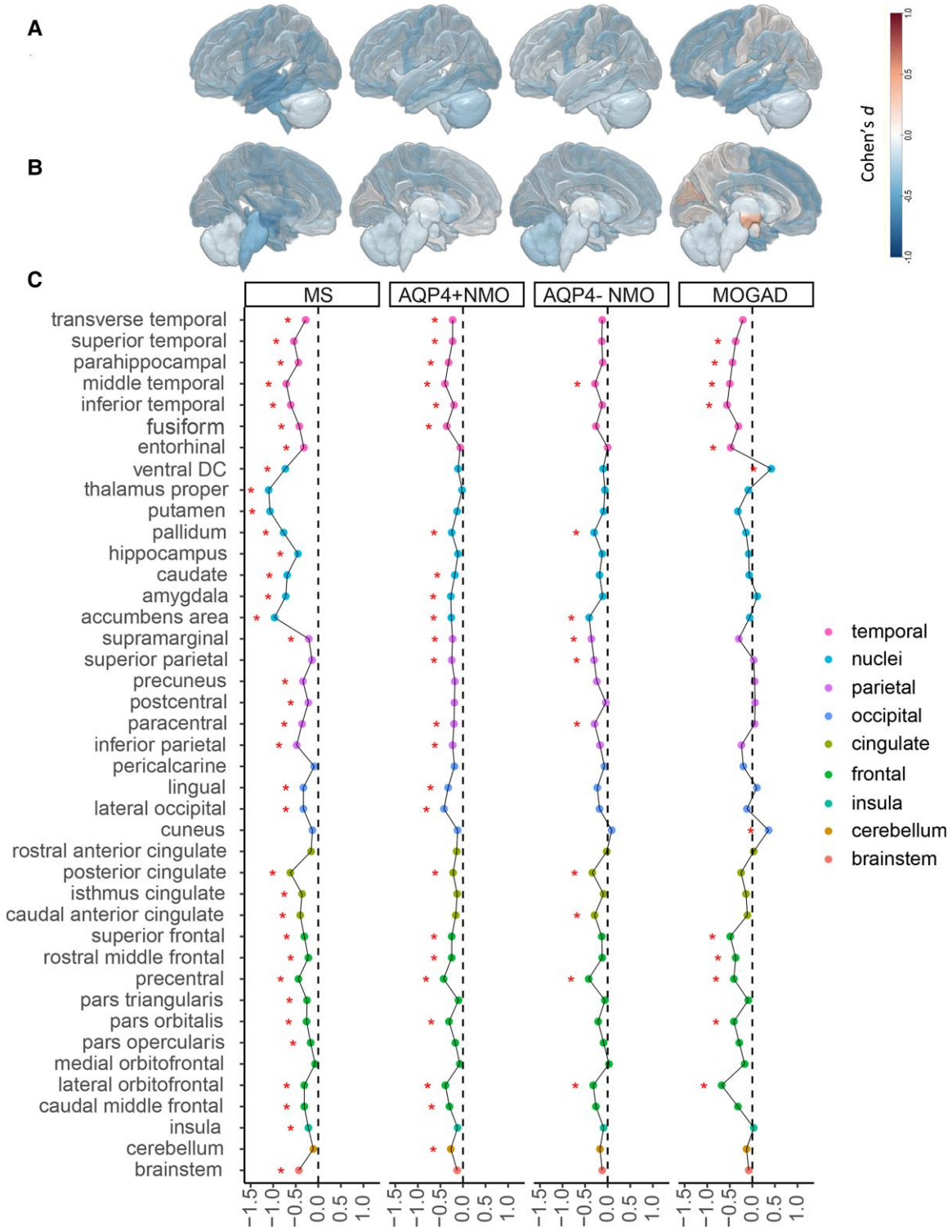

Figure 1 Cohen's *d* values of grey matter atrophy across 41 brain regions in patients with multiple sclerosis, anti-AQP4 antibody-positive (AQP4+ and AQP4– neuromyelitis optica spectrum disorder (NMOSD) and MOG antibody-associated disease (MOGAD) compared with healthy controls. (**A** and **B**) Cohen's *d* mapping of grey matter (GM) atrophy profiles in patients with multiple sclerosis, AQP4+ NMOSD, AQP4– NMOSD and MOGAD. (**C**) Cohen's *d* values of GM atrophy profiles of the four neuroinflammatory diseases. The brain regions with statistically significant atrophy are marked with an asterisk ($P_{FDR} < 0.05$). FDR = false discovery rate.

PC1 exhibited a negative correlation with the GM atrophy profile in each disorder, with multiple sclerosis showing the weakest correlation. PC2 exhibited a strongly positive correlation with the GM atrophy profile of multiple sclerosis [Fig. 3B(i–viii)]. For PC1, interregional variation in the expression of genes specific to microglia, oligodendrocytes and endothelial cells was negatively associated with the GM atrophy profile ($-0.070 < r < -0.067$, $P_{FDR} < 10^{-5}$; Fig. 3C). For PC2, interregional variation in the expression of genes specific to

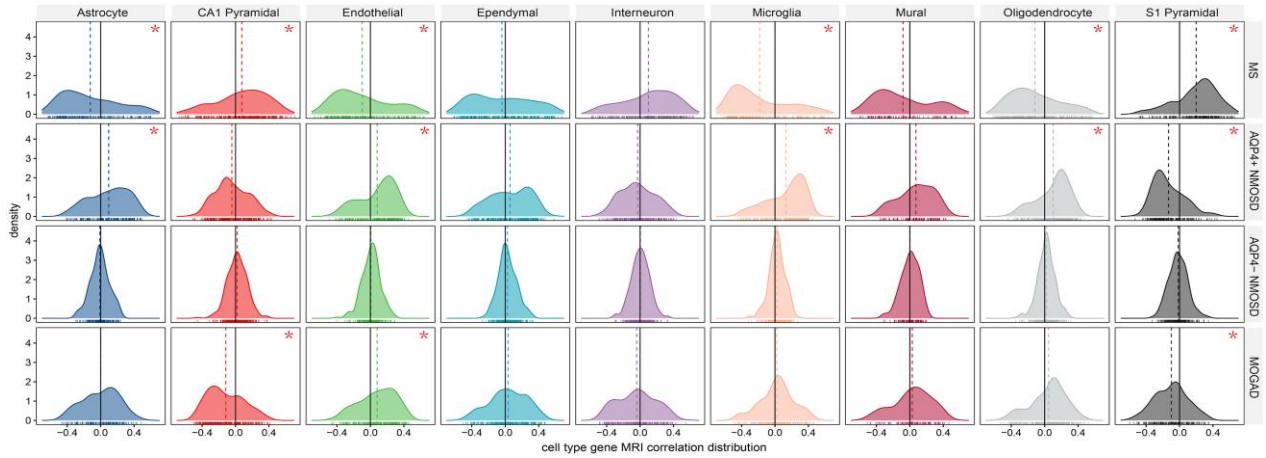

Figure 2 Virtual histology results of grey matter atrophy profiles in patients with multiple sclerosis, anti-AQP4 antibody-positive (AQP4+) and -negative (AQP4–) neuromyelitis optica spectrum disorder (NMOSD) and MOG antibody-associated disease (MOGAD). The cell types exhibiting a statistically significant correlation with grey matter (GM) atrophy profiles are marked with an asterisk ($P_{FDR} < 10^{-5}$). FDR = false discovery rate.

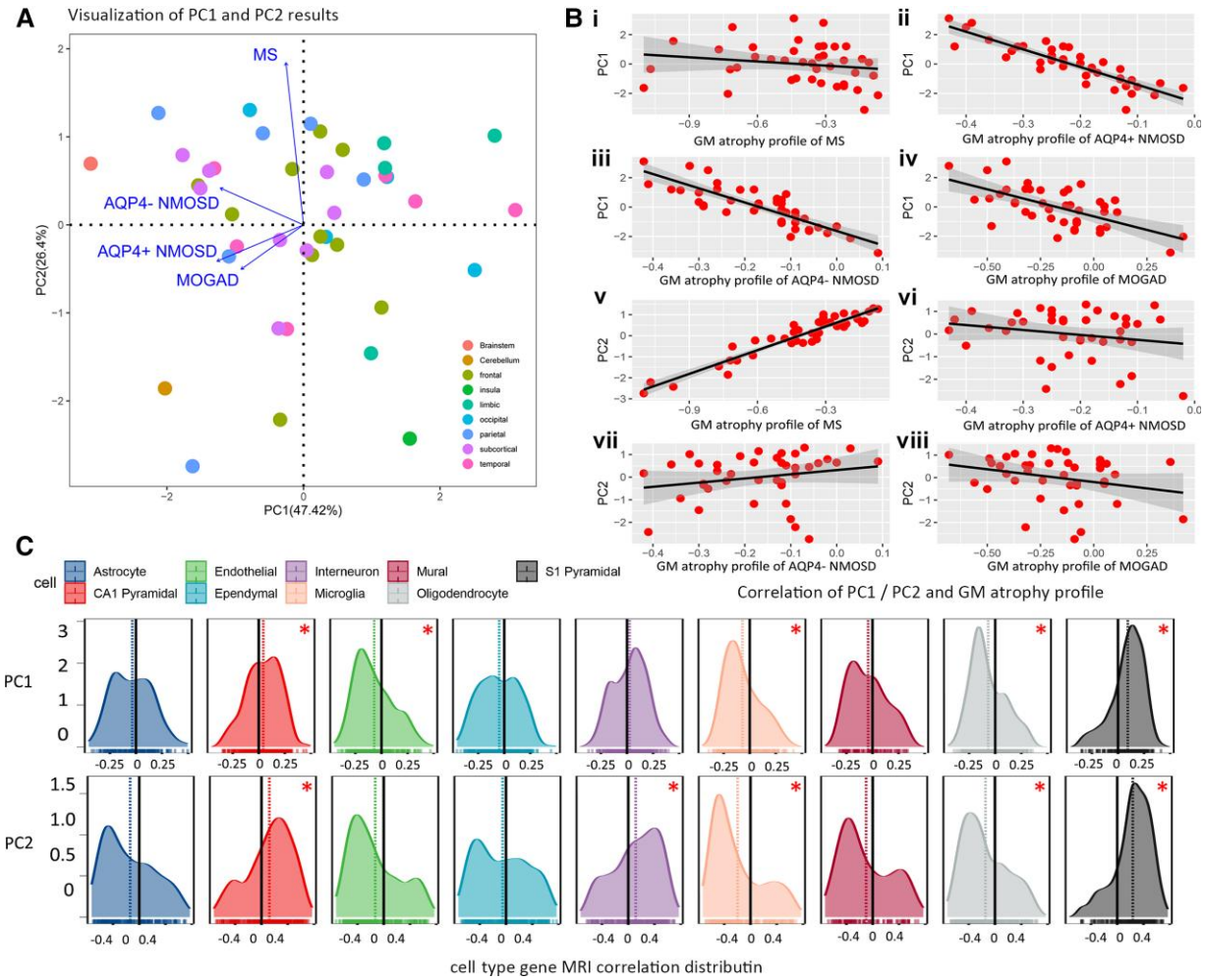

Figure 3 Principal component (PC) analysis results and virtual histology results of PC1 and PC2 for the four neuroinflammatory diseases. (**A**) Visualization of PC1 and PC2 variables. [**B(i–viii)**] The correlations between the PC1/PC2 and the grey matter (GM) atrophy profiles of the four neuroinflammatory diseases. Multiple sclerosis showed most relevance to PC2 but least relevance to PC1. Anti-AQP4 antibody-positive (AQP4+) and -negative (AQP4–) neuromyelitis optica spectrum disorder (NMOSD) and MOG antibody-associated disease (MOGAD) showed most relevance to PC1 but least relevance to PC2. (**C**) Virtual histology results of PC1 and PC2 of GM atrophy profiles in the four neuroinflammatory diseases.

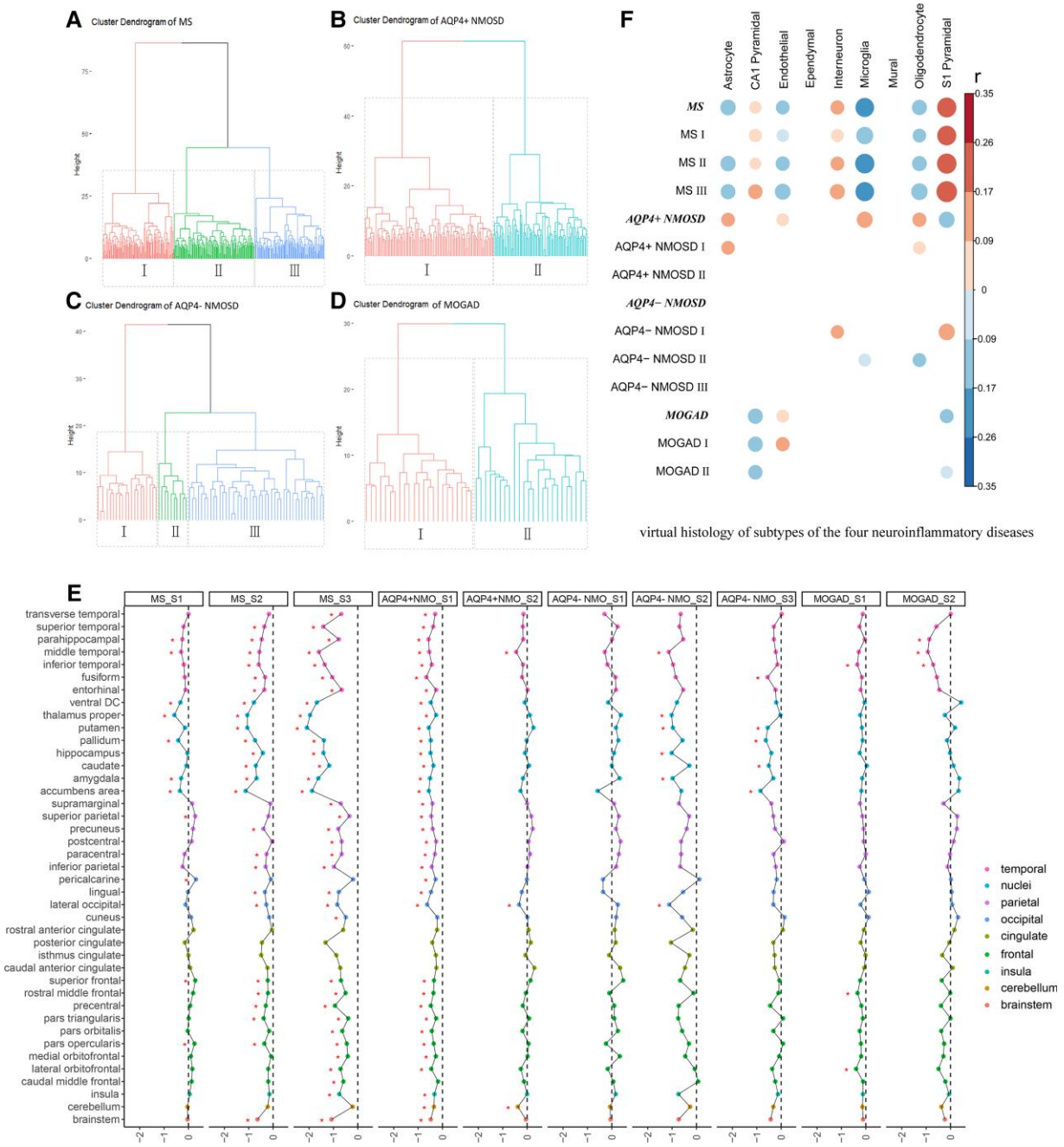

Figure 4 Hierarchical clustering results and virtual histology results of the subtypes in the four neuroinflammatory diseases. (**A**) Multiple sclerosis was grouped into three subtypes. (**B**) Anti-AQP4 antibody-positive (AQP4+) neuromyelitis optica spectrum disorder (NMOSD) was grouped into two subtypes. (**C**) Anti-AQP4 antibody-negative AQP4– NMOSD was grouped into three subtypes. (**D**) MOG antibody-associated disease (MOGAD) was grouped into two subtypes. (**E**) Cohen's *d* values among 41 brain regions in the subtypes of the four neuroinflammatory diseases. The brain regions with statistically significant atrophy are marked with an asterisk ($P_{FDR} < 0.05$). (**F**) Virtual histology results of the grey matter (GM) atrophy profiles in the subtypes of the four neuroinflammatory diseases. Only coefficients with $P_{FDR} < 10^{-5}$ are displayed. FDR = false discovery rate.

microglia and oligodendrocytes were negatively associated with the GM atrophy profile ($-0.196 < r < -0.144$, $P_{FDR} < 10^{-5}$; Fig. 3C).

For subtypes I–III of multiple sclerosis, interregional variation in the expression of genes specific to astrocytes, oligodendrocytes, endothelial and microglial was negatively associated with the inter regional GM atrophy profile ($-0.196 < r < -0.043$, $P_{FDR} < 10^{-5}$; Fig. 4). For subtypes I–III of AQP4– NMOSD, interregional variation in the expression of genes specific to oligodendrocytes and microglial cells was negatively associated with the interregional GM atrophy profile ($-0.082 < r < -0.095$, $P_{FDR} < 10^{-5}$; Fig. 4). For subtypes I–II of MOGAD, interregional variation in the expression of genes specific to CA1 and S1 pyramidal cells was negatively associated with the interregional GM atrophy profile ($-0.116 < r < -0.080$, $P_{FDR} < 10^{-5}$; Fig. 4). No specific CNS cell types were negatively associated with the interregional GM atrophy profile for subtypes I–II of AQP4+ NMOSD.

Virtual histology of clinical features associated grey matter atrophy

As regional GM volume in the four neuroinflammatory diseases was associated with EDSS, disease duration, relapse number, lesion volume and MoCA (Supplementary Fig. 3), we also characterized GM atrophy profiles based on these clinical features across 41 regions. The multiple sclerosis patients with high EDSS scores showed more GM atrophy in subcortical nuclei than patients with low EDSS scores (Fig. 5). The AQP4– NMOSD patients with multiple relapses showed obvious GM atrophy in parietal cortex than patients with single relapse. The MOGAD patients with low MoCA scores showed more GM atrophy in temporal and frontal cortices than those with high MoCA scores (Fig. 5).

In patients with multiple sclerosis, interregional variation in the expression of genes specific to endothelial cells, oligodendrocytes, astrocytes, ependymal cells and microglia was negatively correlated with the EDSS associated GM atrophy profile ($-0.089 < r < -0.066$,

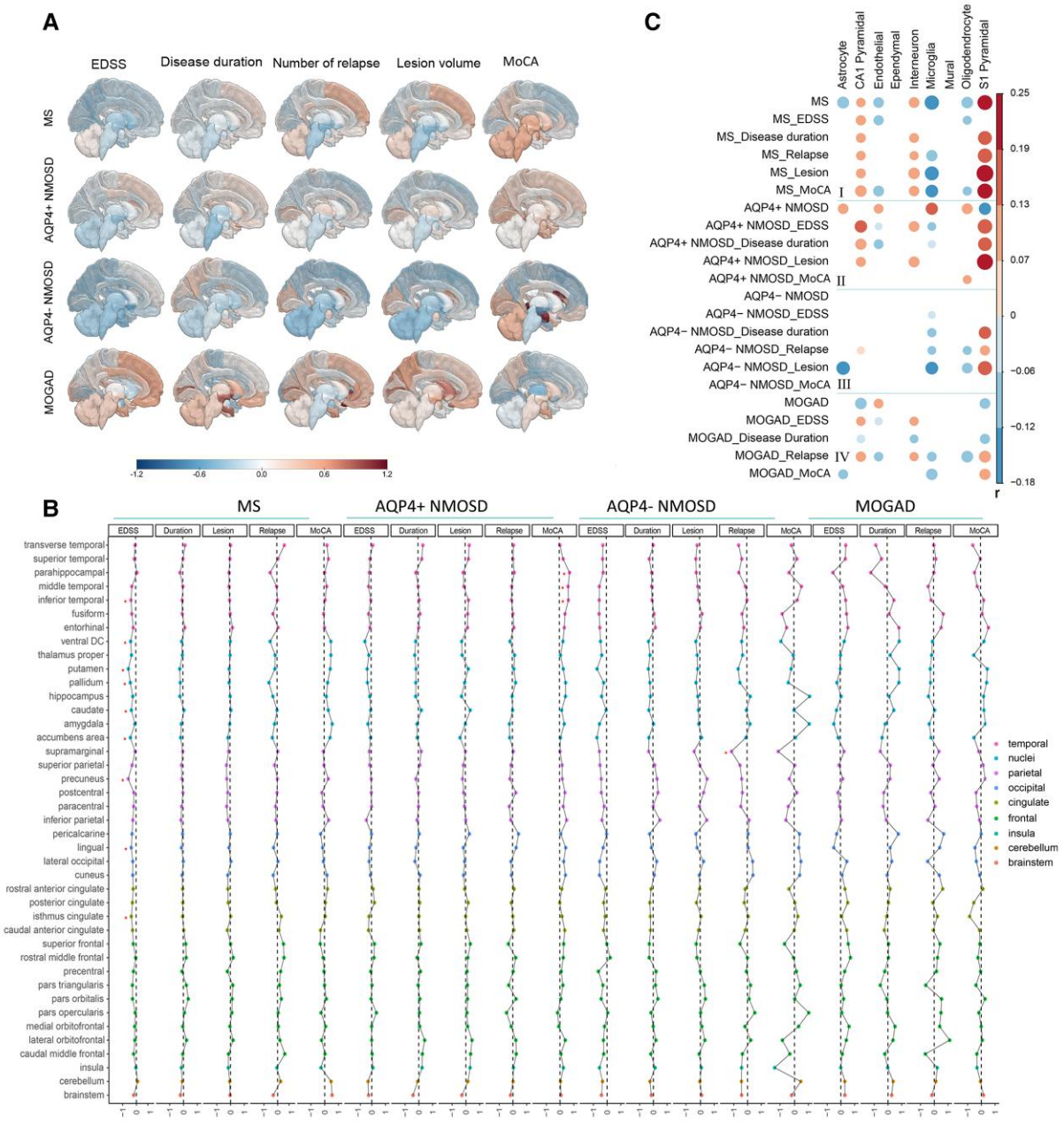

Figure 5 Cohen's *d* values of grey matter atrophy in patients with multiple sclerosis, anti-AQP4 antibody-positive (AQP4+) and -negative (AQP4–) neuromyelitis optica spectrum disorder (NMOSD) and MOG antibody-associated disease (MOGAD) grouped by clinical features and their virtual histology results. (**A**) Cohen's *d* mapping of grey matter (GM) atrophy in patients with the four neuroinflammatory diseases grouped by clinical features. (**B**) Cohen's *d* values of GM atrophy in patients with the four neuroinflammatory diseases grouped by clinical features. (**C**) Virtual histology results of GM atrophy profiles based on clinical features in patients with multiple sclerosis, AQP4+ NMOSD, AQP4– NMOSD and MOGAD. Only coefficients with $P_{FDR} < 10^{-5}$ are displayed. The size and colour of each circle represents the coefficient. EDSS = Expanded Disability Status Scale; FDR = false discovery rate; MoCA = Montreal Cognitive Assessment.

$P_{FDR} < 10^{-5}$; Fig. 5 and Supplementary Table 3). In patients with AQP4 – NMOSD, interregional variation in the expression of genes specific to oligodendrocytes and microglia were negatively associated with the relapse number associated GM atrophy profile ($-0.067 < r < -0.065$, $P_{FDR} < 10^{-5}$; Fig. 5 and Supplementary Table 5). In patients with MOGAD, interregional variation in the expression of genes specific to S1 pyramidal cells was negatively associated with the MoCA associated GM atrophy profile ($r = -0.108$, $P_{FDR} < 10^{-5}$; Fig. 5 and Supplementary Table 7) (detailed in the Supplementary material, 'Results' section).

Discussion

We used a virtual histology approach to identify the putative pathophysiological basis of interregional differences in GM atrophy profiles among patients with multiple sclerosis, AQP4+ NMOSD, AQP4– NMOSD and MOGAD (Figs 1 and 2 and Supplementary Tables 1 and 2). Furthermore, the intrasession and intersession variations of GM atrophy in the four neuroinflammatory diseases were analysed by PCA and hierarchical clustering analysis, along with virtual histology analysis (Figs 3 and 4). Then, we explored the histology of clinical relevant atrophy by subgroup analysis that stratified by physical disability, disease duration, number of relapses, lesion burden and cognitive function (Fig. 5, Supplementary Fig. 3 and Supplementary Tables 3–7). Our findings provide a comprehensive understanding of the underlying histology of GM atrophy profiles for neuroinflammatory diseases, with important implications for targeted clinical medicine.

Grey matter atrophy patterns in the four neuroinflammatory diseases

It has been reported that multiple sclerosis patients show lower cortical and subcortical GM volumes than healthy controls[12,28] and more sever thalamus atrophy[13] and brainstem atrophy[17] than NMOSD patients. This aligned with our finding that multiple sclerosis showed severe widespread atrophy, especially in subcortical cortex and brainstem compared with AQP4+ NMOSD, AQP4– NMOSD and MOGAD based on a multicentre cohort. Thus, the finding of a multiple sclerosis atrophy pattern was rational. AQP4+ NMOSD has previously been associated with a decreased cortical GM volume without subcortical atrophy.[12] However, AQP4+ NMOSD showed cortical GM atrophy and partial atrophy of subcortical nuclei in our study. This may be due to the larger sample size in the current study, which was used to increase statistical power and sensitivity. Moreover, we found that AQP4+ NMOSD showed atrophy in occipital cortex compared with MOGAD, which also agreed with the more severe visual symptoms seen in NMOSD.[29] Finally, MOGAD showed atrophy in temporal and frontal cortices compared with healthy controls, AQP4+ NMOSD and AQP4– NMOSD in this study, which is supported by previous studies.[12,13] Although different amounts of GM volume loss have been reported previously in patients with multiple sclerosis, AQP4+ NMOSD and MOGAD,[3,12-14,17] we have provided detailed regional GM atrophy profiles using data from a multicentre cohort.

Different virtual histology underlying grey matter atrophy patterns of four neuroinflammatory diseases

In multiple sclerosis, high gene expression levels specific to microglia, astrocytes, oligodendrocytes and endothelial cells predominantly correlated with GM atrophy profiles, whereby enrichment analysis revealed similar upregulated metabolic processes related to nucleic acid or RNA, as well as downregulated immune processes (Supplementary material, 'Methods' section and Supplementary Fig. 4). The activation of glial cells is widely believed to be associated with the occurrence and progression of multiple sclerosis[15]; however, our results indicate that endothelial cells cannot be ignored in GM atrophy of multiple sclerosis. Disruption to endothelial cells increases the permeability of the blood–brain barrier and leads to a switch from superficial layer neurogenesis to gliogenesis, thereby resulting in decreased neuronal numbers.[30] Furthermore, endothelial dysfunction is believed to be responsible for vascular abnormalities and ischemic stroke in multiple sclerosis.[31,32] In clinical practice, the treatment of vascular risk factors can help delay the progression of neurodegenerative diseases such as Alzheimer's disease.[33] Together, this indicates that both glial and endothelial cells should be considered potential targets for GM atrophy in multiple sclerosis.

In AQP4+ NMOSD and MOGAD, high gene expression specific to CA1 pyramidal cells predominantly contributed to the GM atrophy profile, which is mainly located in the hippocampus. Enrichment analysis revealed upregulated RNA metabolism and cell movement and migration, as well as downregulated nervous system development processes in MOGAD (Supplementary material, 'Methods' section, and Supplementary Fig. 4). Meanwhile, the hippocampus was not atrophied in both diseases. These findings indicated that hippocampal neurons might contribute to the maintenance of volume through neurorestoration in patients with AQP4+ NMOSD and MOGAD. The immunoglobulin G autoantibody of AQP4 is typical among AQP4+ NMOSD patients; it targets astrocytes characterized by the enrichment of APQ4 on the membrane surface. Therefore, our reported low gene expression levels of astrocytes in AQP4+ NMOSD was a rational finding, which is also supported by previous literature.[34]

In MOGAD, the expression of MOG on the surface of oligodendrocytes may result in brain atrophy by augmenting demyelination,[11] which also leads to endothelial cell dysfunction.[35,36] This agrees with our finding that low expression levels of endothelial cell-specific genes are responsible for GM atrophy in MOGAD. The partial effectiveness of anti-inflammatory therapies for AQP4+ NMOSD and MOGAD also suggests that protecting target neurons and vessels might be necessary. Indeed, with Alzheimer's disease therapy, it has been shown that the regulation of glutamate homeostasis can protect hippocampal neurons,[37] which might also be effective in NMOSD and MOGAD. No CNS cells were identified in the virtual histology of the GM atrophy profile for AQP4– NMOSD, which might be caused by the high heterogeneity of this disease.

Furthermore, we noticed opposing patterns in the virtual histology of the GM atrophy profiles between multiple sclerosis and its mimics. High expression levels of genes (specific to microglia, astrocytes, oligodendrocytes and endothelial cells), which drove the GM atrophy profile in multiple sclerosis, were expressed at low levels in AQP4+ NMOSD and MOGAD. Conversely, high expression levels of genes (specific to S1 and CA1 pyramidal cells), which were linked to the GM atrophy profiles in NMOSD and MOGAD, were expressed at low levels in multiple sclerosis. This indicated that their optimal therapeutic approaches may differ. This notion is consistent with clinical practice, that most multiple sclerosis disease-modifying drugs (such as beta-interferons, glatiramer acetate, natalizumab, alemtuzumab, fingolimod and dimethyl-fumarate) are not only ineffective in NMOSD[22] and MOGAD[38] but cause disease exacerbation in NMOSD.[22] Our virtual histology results provide deeper understanding of the pathologies of these four neuroinflammatory diseases and suggest new therapeutic directions.

Virtual histology of principal component analysis and hierarchical clustering results

Based on the PCA results, the disparity in GM atrophy profiles among the four neuroinflammatory diseases could be differentiated by the interregional patterns and distinct gene expression levels in neurons (Fig. 3). PC1 was negatively associated with the GM atrophy profile of AQP4+ NMOSD, AQP4– NMOSD and MOGAD, and its virtual histology reverse to the virtual histology of AQP4+ NMOSD and MOGAD. PC2 was positively associated with the GM atrophy profile of multiple sclerosis, and its virtual histology aligned with the virtual histology of multiple sclerosis. Furthermore, the PC1 and PC2 could be differentiated by endothelial and interneuron cells. This implied that the intrasession variations of GM atrophy profiles in the four neuroinflammatory diseases could be explained by the endothelial cell and neuron damage.

The hierarchical clustering analysis indicated that the four inflammatory diseases could be grouped into subtypes, which displayed the intersession variations of GM atrophy profiles in four neuroinflammatory diseases (Fig. 4). Although the GM atrophy patterns of subtypes were distinct, their virtual histologies were not changed when compared with the virtual histology of all cases of the four neuroinflammatory diseases. This suggested the virtual histology results of this study were not affected by disease heterogeneity.

Virtual histology of clinical feature-associated GM atrophy profiles varies across four diseases

The EDSS-associated GM atrophy patterns were characteristic in subcortical areas in multiple sclerosis, as displayed in Fig. 5. In multiple sclerosis, the virtual histology results for EDSS-associated GM atrophy were similar to the virtual histology of the GM atrophy compared to healthy controls, suggesting that GM atrophy is the characteristic of EDSS progression in multiple sclerosis. This phenomenon was absent in AQP4+ NMOSD, AQP4– NMOSD and MOGAD. In addition, the gene expression of CA1 pyramidal cells, which are predominantly located in the hippocampus, was suppressed in EDSS-associated GM atrophy. The hippocampus undergoes significant atrophy in multiple sclerosis (Fig. 1). This indicated that the neuron damage shown to underlie EDSS-associated GM atrophy was reliable. Anti-inflammatory therapies currently used to treat multiple sclerosis exhibit partial efficacy at the early disease stage. However, their effectiveness is limited during the progressive phase, which is probably dominated by cytodegenerative processes (of neurons, axons and oligodendrocytes).[15] Therefore, we suggest that neuronal cells, in addition to glial cells, should be targeted for multiple sclerosis treatments.

In AQP4– NMOSD, the GM atrophy patterns based on relapse number are characteristic in the parietal area (Fig. 5). However, we found that no CNS cells were responsible for GM atrophy in any AQP4– NMOSD cases, but low gene expression specific to neuron cells and high gene expression specific to glial cells were highlighted by the level of relapse-associated GM atrophy. Current medical treatments for NMOSD attempt to reduce ongoing inflammation and prevent future relapses.[22] Therefore, we speculate that the poor outcome following attacks in patients with AQP4– NMOSD might be associated with a lack of neuronal protection, which might occur at the initial stage of the neuro-restoration process.

Similarly, in MOGAD, the GM atrophy patterns based on the MoCA are characteristic in frontal and temporal cortices (Fig. 5). MoCA-related GM atrophy profiles exhibited completely different virtual histology patterns to those of the GM atrophy profiles of all cases with MOGAD. Genes specific to CA1 and S1 pyramidal cells, which were expressed highly in the GM atrophy profile of all MOGAD cases were expressed at low levels in the MoCA progression-associated GM atrophy profile. Genes specific to endothelial cells, which were expressed at low levels in the GM atrophy profile of all cases in MOGAD, were highly expressed in the MoCA progression-associated GM atrophy profile. This observation also suggested the possibility of neuronal and endothelial cell impairment underlying MoCA progression-related GM atrophy. The reversal of virtual histology findings may be linked to the phenomenon of lesion migration in MOGAD.[39]

Anti-inflammatory therapy has been reported to be efficacious in managing acute episodes of neuroinflammatory diseases.[38,40,41] This study provides additional evidence concerning shared and distinct neuroimaging and pathophysiological characteristics of GM atrophy among four neuroinflammatory diseases, which may help their differential diagnoses and guide optimal therapeutic strategies.

Limitations

There are several limitations to our study. First, the multicentre cohort included patients and healthy controls from several local institutes, and many external healthy controls from a public database. Heterogeneity exists in both clinical diagnoses and MRI acquisition, despite our corrections for site-related effects. To exclude the influence of heterogeneity, we analysed the virtual histology of subgroups using the hierarchical clustering results. The virtual histology results of the subtypes were consistent with the findings in the four neuroinflammatory diseases (Fig. 4). Second, we observed different GM atrophy patterns with distinct virtual histology among the four inflammatory diseases. However, we were only able to speculate on their potential pathologies using the metrics of their GM atrophy profiles. These findings should be further validated using more specific *in vivo* imaging techniques and animal experiments.[15] Third, the AHBA microarray dataset that was used contains brain-wide gene expression measurements for 3702 brain region samples from the post-mortem brains of six healthy adults. Despite this limitation, the statistical methods used in this study to link GM differences to gene expression have previously been demonstrated to be statistically robust.[31] Lending further confidence to our results, our virtual histology results replicated previous cross-validation analyses, and analysis of PubMed abstracts provided further support.[42,43] The PCA results also illustrated the stability of the virtual histology methods (Fig. 3). Future studies based on longitudinal data will provide a better understanding of the dynamic transcriptional signatures of histology mechanisms.

Conclusions

In summary, multiple sclerosis showed severe widespread GM atrophy, mainly involving subcortical nuclei and the brainstem. AQP4+ NMOSD showed obvious widespread GM atrophy, predominately located in the occipital cortex and cerebellum. AQP4– NMOSD showed mild widespread GM atrophy, mainly located in the frontal and parietal cortices. MOGAD showed GM atrophy mainly involving the frontal and temporal cortices. Their unique underlying virtual histology patterns were microglia, astrocytes and oligodendrocytes for multiple sclerosis; astrocytes for AQP4+ NMOSD; and oligodendrocytes for MOGAD. Neuronal and endothelial cells were shared potential targets across these neuroinflammatory diseases.

Data availability

Data that support the findings of this study are available from the corresponding author, upon reasonable request.

Acknowledgements

We would like to thank Rachel James and Yifei Zhang (GE Healthcare) for editing a draft of this manuscript.

Funding

This study has received funding by Beijing Municipal Natural Science Foundation for distinguished Young Scholars (JQ20035); National Science Foundation of China (81571631, 81870958, 82202084 and 82330057); Beijing Municipal Natural Science Foundation (7244328); Young Scientist Project, Beijing Tiantan Hospital, Capital Medical University (ZZZ); Beijing Hospital Management Center Young Talents (QML20210505); China Postdoctoral Science Foundation (2022M712221).

Competing interests

The authors report no competing interests.

Supplementary material

Supplementary material is available at *Brain* online.

References

1. Mahad DH, Trapp BD, Lassmann H. Pathological mechanisms in progressive multiple sclerosis. *Lancet Neurol*. 2015;14:183-193.
2. Reindl M, Waters P. Myelin oligodendrocyte glycoprotein antibodies in neurological disease. *Nat Rev Neurol*. 2019;15:89-102.
3. Zhuo Z, Duan Y, Tian D, et al. Brain structural and functional alterations in MOG antibody disease. *Mult Scler*. 2021;27:1350-1363.
4. James RE, Schalks R, Browne E, et al. Persistent elevation of intrathecal pro-inflammatory cytokines leads to multiple sclerosis-like cortical demyelination and neurodegeneration. *Acta Neuropathol Commun*. 2020;8:66.
5. Bajrami A, Magliozzi R, Pisani AI, et al. Volume changes of thalamus, hippocampus and cerebellum are associated with specific CSF profile in MS. *Mult Scler*. 2021;28:550-560.
6. Kawachi I, Lassmann H. Neurodegeneration in multiple sclerosis and neuromyelitis optica. *J Neurol Neurosurg Psychiatry*. 2017;88:137-145.
7. Hinson SR, Roemer SF, Lucchinetti CF, et al. Aquaporin-4-binding autoantibodies in patients with neuromyelitis optica impair glutamate transport by down-regulating EAAT2. *J Exp Med*. 2008;205:2473-2481.
8. Geis C, Ritter C, Ruschil C, et al. The intrinsic pathogenic role of autoantibodies to aquaporin 4 mediating spinal cord disease in a rat passive-transfer model. *Exp Neurol*. 2015;265:8-21.
9. Lucchinetti CF, Mandler RN, McGavern D, et al. A role for humoral mechanisms in the pathogenesis of Devic's neuromyelitis optica. *Brain*. 2002;125:1450-1461.
10. Hokari M, Yokoseki A, Arakawa M, et al. Clinicopathological features in anterior visual pathway in neuromyelitis optica. *Ann Neurol*. 2016;79:605-624.
11. Höftberger R, Guo Y, Flanagan EP, et al. The pathology of central nervous system inflammatory demyelinating disease accompanying myelin oligodendrocyte glycoprotein autoantibody. *Acta Neuropathol*. 2020;139:875-892.
12. Duan Y, Zhuo Z, Li H, et al. Brain structural alterations in MOG antibody diseases: A comparative study with AQP4 seropositive NMOSD and MS. *J Neurol Neurosurg Psychiatry*. 2021;92:709-716.
13. Liu Y, Duan Y, Huang J, et al. Multimodal quantitative MR imaging of the thalamus in multiple sclerosis and neuromyelitis optica. *Radiology*. 2015;277:784-792.
14. Liu Y, Fu Y, Schoonheim MM, et al. Structural MRI substrates of cognitive impairment in neuromyelitis optica. *Neurology*. 2015;85:1491-1499.
15. Klaver R, De Vries HE, Schenk GJ, Geurts JJ. Grey matter damage in multiple sclerosis: A pathology perspective. *Prion*. 2013;7:66-75.
16. Spence RD, Kurth F, Itoh N, et al. Bringing CLARITY to gray matter atrophy. *Neuroimage*. 2014;101:625-632.
17. Messina S, Mariano R, Roca-Fernandez A, et al. Contrasting the brain imaging features of MOG-antibody disease, with AQP4-antibody NMOSD and multiple sclerosis. *Mult Scler*. 2022;28:217-227.
18. Natu VS, Gomez J, Barnett M, et al. Apparent thinning of human visual cortex during childhood is associated with myelination. *Proc Natl Acad Sci U S A*. 2019;116:20750-20759.
19. Carlo CN, Stevens CF. Structural uniformity of neocortex, revisited. *Proc Natl Acad Sci U S A*. 2013;110:1488-1493.
20. Vidal-Pineiro D, Parker N, Shin J, et al. Cellular correlates of cortical thinning throughout the lifespan. *Sci Rep*. 2020;10:21803.
21. Pelvig DP, Pakkenberg H, Stark AK, Pakkenberg B. Neocortical glial cell numbers in human brains. *Neurobiol Aging*. 2008;29:1754-1762.
22. Kira JI. Unexpected exacerbations following initiation of disease-modifying drugs in neuromyelitis optica spectrum disorder: Which factor is responsible, anti-aquaporin 4 antibodies, B cells, Th1 cells, Th2 cells, Th17 cells, or others? *Mult Scler*. 2017;23:1300-1302.
23. Shin J, French L, Xu T, et al. Cell-specific gene-expression profiles and cortical thickness in the human brain. *Cereb Cortex*. 2018;28:3267-3277.
24. Patel Y, Shin J, Drakesmith M, Evans J, Pausova Z, Paus T. Virtual histology of multi-modal magnetic resonance imaging of cerebral cortex in young men. *Neuroimage*. 2020;218:116968.
25. Writing Committee for the Attention-Deficit/Hyperactivity DisorderAutism Spectrum DisorderBipolar Disorder, et al. Virtual histology of cortical thickness and shared neurobiology in 6 psychiatric disorders. *JAMA Psychiatry*. 2021;78:47-63.
26. Arnatkevičiūtė A, Fulcher BD, Fornito A. A practical guide to linking brain-wide gene expression and neuroimaging data. *Neuroimage*. 2019;189:353-367.
27. Zeisel A, Muñoz-Manchado AB, Codeluppi S, et al. Brain structure: Cell types in the mouse cortex and hippocampus revealed by single-cell RNA-seq. *Science*. 2015;347:1138-1142.
28. Lee CY, Mak HK, Chiu PW, Chang HC, Barkhof F, Chan KH. Differential brainstem atrophy patterns in multiple sclerosis and neuromyelitis optica spectrum disorders. *J Magn Reson Imaging*. 2018;47:1601-1609.
29. Etemadifar M, Sabeti F, Ebrahimian S, Momeni F. Dorsal midbrain involvement in MRI as a core clinical manifestation for NMOSD diagnosis. *Mult Scler Relat Disord*. 2020;43:102150.
30. Wang W, Su L, Wang Y, Li C, Ji F, Jiao J. Endothelial cells mediated by UCP2 control the neurogenic-to-astrogenic neural stem cells fate switch during brain development. *Adv Sci (Weinh)*. 2022;9:e2105208.

31. D'haeseleer M, Cambron M, Vanopdenbosch L, De Keyser J. Vascular aspects of multiple sclerosis. *Lancet Neurol*. 2011;10:657-666.
32. Buch S, Subramanian K, Jella PK, et al. Revealing vascular abnormalities and measuring small vessel density in multiple sclerosis lesions using USPIO. *Neuroimage Clin*. 2021;29:102525.
33. Snyder HM, Corriveau RA, Craft S, et al. Vascular contributions to cognitive impairment and dementia including Alzheimer's disease. *Alzheimers Dement*. 2015;11:710-717.
34. Takai Y, Misu T, Suzuki H, et al. Staging of astrocytopathy and complement activation in neuromyelitis optica spectrum disorders. *Brain*. 2021;144:2401-2415.
35. Miyamoto N, Pham LD, Seo JH, Kim KW, Lo EH, Arai K. Crosstalk between cerebral endothelium and oligodendrocyte. *Cell Mol Life Sci*. 2014;71:1055-1066.
36. Rajani RM, Williams A. Endothelial cell-oligodendrocyte interactions in small vessel disease and aging. *Clin Sci (Lond)*. 2017;131:369-379.
37. Danysz W, Parsons CG. Glycine and N-methyl-D-aspartate receptors: Physiological significance and possible therapeutic applications. *Pharmacol Rev*. 1999;50:597-664.
38. Hacohen Y, Wong YY, Lechner C, et al. Disease course and treatment responses in children with relapsing nyelin oligodendrocyte glycoprotein antibody-associated disease. *JAMA Neurol*. 2018;75:478-487.
39. Marignier R, Hacohen Y, Cobo-Calvo A, et al. Myelin-oligodendrocyte glycoprotein antibody-associated disease. *Lancet Neurol*. 2021;20:762-772.
40. Zheng F, Li Y, Zhuo Z, et al. Structural and functional hippocampal alterations in multiple sclerosis and neuromyelitis optica spectrum disorder. *Mult Scler*. 2022;28:707-717.
41. Jitprapaikulsan J, Chen JJ, Flanagan EP, et al. Aquaporin-4 and myelin oligodendrocyte glycoprotein autoantibody status predict outcome of recurrent optic neuritis. *Ophthalmology*. 2018;125:1628-1637.
42. Buch AM, Vértes PE, Seidlitz J, Kim SH, Grosenick L, Liston C. Molecular and network-level mechanisms explaining individual differences in autism spectrum disorder. *Nat Neurosci*. 2023;26:650-663.
43. Arnatkeviciute A, Markello RD, Fulcher BD, Misic B, Fornito A. Toward best practices for imaging transcriptomics of the human brain. *Biol Psychiatry*. 2023;93:391-404.